

Modeling of ZnO Nanorods on Paper Substrate for Energy Harvesting

Geetha P 

Professor, Department of Electronics and Communication Engineering, Sree Vidyanikethan Engineering College, Tirupati, India, mailpgeetha2013@gmail.com

*Corresponding Author: Geetha P; mailpgeetha2013@gmail.com

ABSTRACT- Nano devices are used for energy generation, storing, and harvesting. Among other metal oxides, ZnO shows high performance in piezoelectric energy generation. In this work, the analysis of the parameter dependency of the amount of energy generated for a piezoelectric material on a paper flexible substrate is done. The load is applied in the shape of lines and alphabets. It is found that the displacement is directly proportional to the generated energy. The role of surface area in producing energy and the distribution of pressure with respect to material strength are added.

General Terms: Material, metal oxides, pattern recognition, piezo electrical energy, pressure.

Keywords: Energy harvesting, flexible substrate, force, piezoelectric, stress, ZnO Nano-rods.

ARTICLE INFORMATION

Author(s): Geeta P;

Received: 25/06/2022; **Accepted:** 30/09/2022; **Published:** 10/11/2022;

E- ISSN: 2347-470X;

Paper Id: IJEER220635;

Citation: 10.37391/IJEER.100433

Webpage-link:

<https://ijeer.forexjournal.co.in/archive/volume-10/ijeer-100433.html>



Publisher's Note: FOREX Publication stays neutral with regard to jurisdictional claims in Published maps and institutional affiliations.

1. INTRODUCTION

The need for generating non-conventional energy is rapidly growing due to global warming as a primary alarming factor for the human race. The energy generating setup is expected to be environmentally friendly, smaller in size, with low power consumption and a simple structure [1]. Femy P. H. and Jayakumar J., in their work, proposed [2] an integrated solar and wind renewable energy source for an electric vehicle. The benefits of environmentally friendly EVs (electric vehicles) that will support the energy needs and the storage systems in transportation are reviewed by [3]. The RF energy harvester proposed by [4] defeats the challenge of nonlinear behavior of rectifying diode in the harvesting circuit. This was achieved by implementing matching network designed with and without parallel capacitance. Power is generated from common human activities like blood pressure, arm motion, and body temperature. A power of 7W was reported in testing a human weighing 154 pounds [5]. The piezoelectric device using nanorods of metal oxides will be the answer to all the above challenges. Moreover, it is not affected by any electromagnetic interference and the electromechanically coupled design model performs well in different configurations. A piezoelectric device has the ability to convert mechanical energy to electrical energy and vice versa [6]. Small and miniature devices are expected to fulfil their power requirements by themselves by self-powering [7] instead of using a supporting battery system. In comparison to other non-

renewable energy resources, the range of piezoelectric energy produced is broad [8]. Further, the initial cost is also higher for sources like solar and wind energy production [9]. As a better replacement, the piezoelectric material produces energy with metal oxide nanorods [10]. In particular, it is zinc oxide nanorods that excel in their performance compared to their counterparts [11] and [12]. In addition to this discussion, the substrate materials play a vital role in energy generation. If the substrate is flexible and economical, then the application becomes abundant [13]. Flexible materials, such as cloth, rubber, metal foils, and paper, aid in energy conversion more than hard substrates. Modeling and simulation optimise the design for developing the device [14] and [15]. In particular, zinc oxide is preferred for its direct wide band gap (3.33eV). This property helps with current flow at room temperature [16]. This paper is a study of the displacement, polarization, and energy generated on zinc oxide nanorods through simulation by the finite element method.

2. METHODOLOGY

The typical construction of the device model is demonstrated as in *figure 1*. Forest of ZnO Nano-rods is developed and grown between flexible plastic-coated paper substrate. The objective of this work is to observe, measure, and analyse the energy generated from the piezoelectric effect.

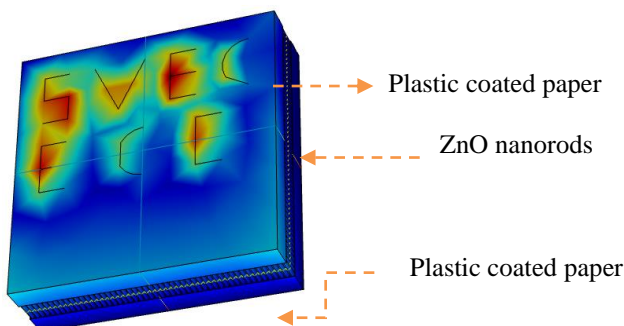


Fig. 1: Schematic diagram of the piezoelectric device model

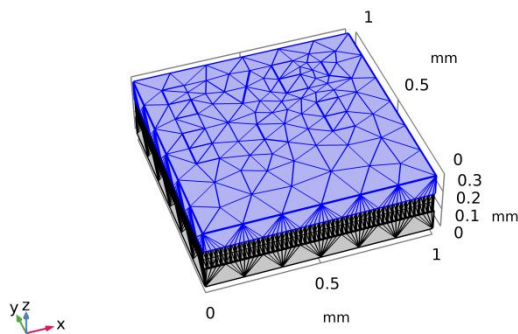


Figure 2: Mesh grid view of the device

The device model created with the Finite Element Method is shown in *figure 1*. ZnO Nano-rods with a 20x20 array, 0.1 mm height, and an 8 nm radius are sandwiched between flexible plastic-coated paper substrates. The paper substrate with plastic coating has a relative permittivity of 3.7. The gadget is subjected to force, and the associated amounts of stored energy and strain are measured. *Figure 2* shows the mesh structure of the device model. The geometry is discretized to model the device in a more effective way with a high aspect ratio using swept meshing. The device is subjected to loads of different pressures at different orientations to study the piezoelectric characteristics. There are two modes of piezoelectric models. d_{33} and d_{31} . In d_{33} mode, the force is applied in vertical direction and in d_{31} mode, the force is applied in horizontal direction. It is illustrated in the *figure 3*.

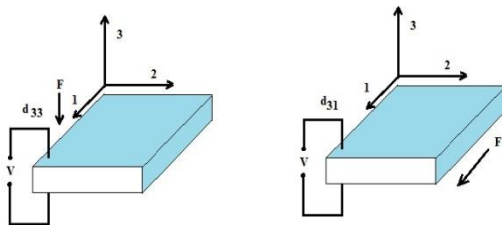


Figure 3: Piezoelectric modes of operation

The purpose of this research is to monitor, quantify, and analyse the energy generated due to the polarisation of piezoelectric zinc oxide nanorods. To do this, the stress, displacement, polarization, and potential of a piezoelectric cylinder are modelled and plotted for various pressures. The device is cut in a line to study the effect on the device cross section. *Table 1* illustrates the electrical properties of plastic-coated paper.

3. RESULTS AND DISCUSSION

The displacement field distribution confirms that sensor stiffness is independent of the shape. Sensing elements that possess the same lateral area could be the next issue in designing the next generation of sensors. The total displacement pattern of the device for an applied pressure of 10^{-3} Nm^2 is shown in *figure 4*. The variation is from 36.25 to $268 \times 10^{-9} \text{ mm}$.

Table 1. Electrical Properties of plastic-coated paper

Compliance Matrix (Pa^{-1}) $\times 10^{-12}$		Coupling Matrix ($\times 10^{-12} \text{ CN}^{-1}$)		Electric Permittivity ($\times 10^{-12} \text{ Fm}^{-1}$)	
S11	2.89	d31	-191	ϵ_{11}	8.15
S12	-9.32	d32	-191	ϵ_{22}	8.15
S13	-5.00	d33	4.95	ϵ_{33}	8.96
S21	2.89	d15	-3.84		
S22	2.82	d24	-3.84		

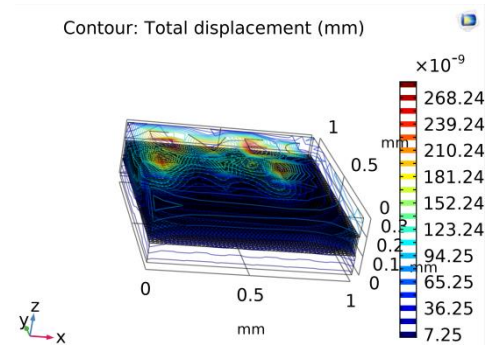


Figure 4: The variation of total displacement in slice view

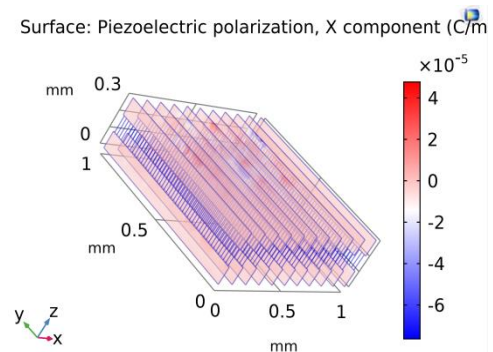


Figure 5: Projection of polarization effect in X component

Polarization is useful to model the electrical bias of the piezoelectric material. The polarization is generated in piezoelectric device for the applied stress. Polarization generates equivalent electric field for enabling the transformation of applied mechanical energy to electrical energy causing electric displacement. It is useful the total electric displacement thus produced can be calculated from

$$D = \epsilon_0 \epsilon_r E + P \quad (1)$$

Where

D is the electric displacement in C/m^2 ,

ϵ is the dielectric strength

E is the electric field strength in Nw/C

P is the polarization C/m .

The binding motion of the strain

$$\epsilon = \frac{\delta}{R_c} \text{ (Bernoulli beam model)} \quad (2)$$

Where,

ϵ – strain

δ – distance of the farthest point to the neutral axis

$\epsilon_{\max} = 0.09$ [4] & [6]

$$\delta = 0.5$$

Then $R_c = 5.5\mu\text{m}$

$$\delta = \frac{t_p}{2}$$

$$Y_{\max} = \frac{0.0151 \cdot PL^4 (1 - N_u^2)}{E_y H^3} \quad (3)$$

Y_{\max} - the maximum displacement

P- Pressure applied

L- length of the diaphragm

N_u -Poisson's ratio

E_y - Young's modulus

H - thickness of diameter

$$V = \frac{d_{33} X f X t}{E_{33} X L X W} \quad (4)$$

V- Potential

d_{33} - piezoelectric charge constant per unit stress applied in direction 3

E_{33} - dielectric constant applied in direction 3

f - Eigen Frequency

t - thickness of piezoelectric patch

L - length of piezoelectric patch

W - Width of piezoelectric patch

The electromechanical coupling coefficient is defined as the conversion of mechanical energy into electrical energy or vice versa. The former is of direct type and the lateral is indirect type. It can be quantified by the following equation (5) and (6).

$$k = \sqrt{\frac{\text{Mechanical energy applied}}{\text{Electrical energy stored}}} \quad (5)$$

$$= \sqrt{\frac{\text{Mechanical energy stored}}{\text{Electrical energy applied}}} \quad (6)$$

Figure 5 is the polarization that resulted with the applied stress. The plot gives the clear variation of the polarization throughout the device. The maximum occurs at $5 \times 10^{-5} \text{ C/m}$ is found.

Figure 6 shows the consolidation of the total displacement the effects of displacement on the electric generated by the nano generator are studied. The height of zinc oxide nanorods is 0.1mm with diameter of 16nm. Number of nanorods are 400 with the 0.1nm distance placed apart from each other. The pressure or load applied displaces the rods to experience a change in the height. The device is sliced to visualize the variation through the device in yz plane.

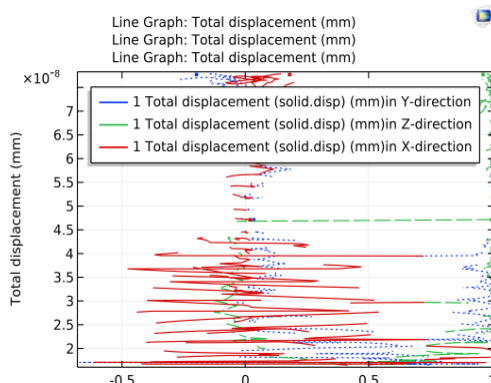


Figure 6: The Dipalcement in the x,y and z- axis

The maximum variation is found through the strokes of letters as $30 \times 10^{-8} \text{ mm}$ with 10 N/m^2 as input and reduces linearly through the structure. The maximum occurs at the surface i.e at $z=0.3 \text{ mm}$, $y= 1 \text{ mm}$ and at $x= 1 \text{ mm}$. The minimum occurs at the surface i.e at $z= -0.5 \text{ mm}$, $y= 0 \text{ mm}$ and at $x= 0 \text{ mm}$. The amount of displacement on top of the zinc rods is more between -0.3 mm to 0.5 mm and results in the generation of -0.16 V . This ensures the piezo electric generation.

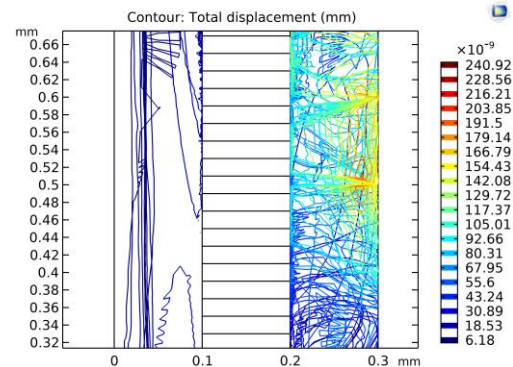


Figure 7: 2D contour plot at the cross section of the device respectively

The 2D graph in figure 7 shows the contour variation of displacement more from 0.2 to 0.3mm of the device. It is the top surface of the device. The distance from 0 to .1 is the bottom substrate block and from 0.1 to 0.2 are the zinc oxide nanorods. The maximum displacement is found to be $240 \times 10^{-9} \text{ mm}$. Figure 8 illustrates the total displacement Vs Floating potential with the cutline at the centre of the device. the electric potential is studied of the device. Table 2 projects the amount of electrical energy values produced from different kinds of force applied.

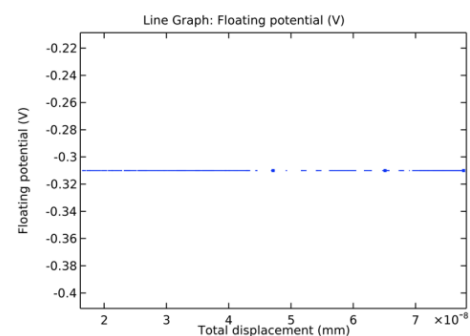


Figure 8: illustration of the total displacement Vs Floating potential

Table 2: List of electrical energy values produced from different kinds of force applied

S.No	Geometry of load	Force applied (N/m ²)	Total strain (fJ)	Total electrical energy obtained (fJ)
1.	Entire surface	100	72.544	52.6754
2.	Block	100	0.028	0.00120
3.	Line	10	110.29	538.971
4.	Alphabet A	10	5215.6	197.302
5.	Array of Letters 'ECE'	10	753.84	256.842
6.	Array of Letters 'SVEC ECE'	10	1623.4	587.671

It is observed that the potential developed for the applied pressure from (0 to 2.5×10^5) is -0.31V with displacement variation from 2 to 7.5×10^{-8} mm. Even though the same amount of force is delivered with both loads, it has been noticed that the energy produced by applying load to the complete block and the entire surface is lower for the block. As a result, the electric energy obtained varies greatly. This leads us to the conclusion that surface area of action is crucial for generating energy.

To check the novelty, this work is compared with the references [6], [7], [9] and [13]. Table 3 provides the comparative study of this work with the reference work. It is observed that the potential developed in this work is greater of all other references for very small stress. but approximates to [6]. It is because of the size and array structure of ZnO nanorods in this work and it is silicon nanowires structure in [6]. So, it is justified that ZnO Nano-structures provides improved performance than Si nanowires.

Table 3: Comparison of the references with this model

S. No.	Reference	Stress (MPa)	Potential Developed (mV)
1.	[6]	116	308
2.	[7]	95	230
3.	[9]	3266	280
4.		3227	672
5.	[13]	0.4	450
6.	This Work	0.00001	317

4. CONCLUSION

The analyses clearly project the dependency of pressure on the displacement and in turn to the electricity generated. More the displacement, more the power generated from the piezoelectric vibration. The energy produced by a load utilizing a line and an alphabet is similar, with the line load producing more energy than the alphabet because of its total length. So, there is great variation in the obtained electric energy. From this it can be concluded that surface area of action plays a vital role in producing the energy. Similarly, from the energy generated by load using line and an alphabet, the line load produces more energy than the alphabet. It is because the length of the line is more than the alphabet length. Despite the same applied force, a separate area is being affected. The surface area of a piezoelectric material that is exposed to force is directly proportional to the energy produced, according to the discussion above. This design and simulation results can be used for signature verification since a potential of 0.3V is generated with a small stress. The generated potential can be taken as reference and be crosschecked for signature verification.

5. ACKNOWLEDGMENTS

This work is done in National MEMS design centre, Sree Vidyanikethan Engineering College, Tirupati.

REFERENCES

[1] Pramod Kumar Sharma, Prashant V. Baredar, "Analysis on piezoelectric energy harvesting small scale device – a review", Journal of King Saud University - Science, Volume 31, Issue 4, 2019, Pages 869-877.

[2] Femy P. H. and Jayakumar J, "A Review on the Feasibility of Deployment of Renewable Energy Sources for Electric Vehicles under Smart Grid Environment", International Journal of Electrical and Electronics Research (IJEER) Volume 9, Issue 3, FOREX Publication, pp:57-65, 2022.

[3] Sachin B. Shahapure, Vandana A. Kulkarni (Deodhar) and Sanjay M. Shinde, "A Technology Review of Energy Storage Systems, Battery Charging Methods and Market Analysis of EV Based on Electric Drives", International Journal of Electrical and Electronics Research (IJEER) , Volume 10, Issue 1, FOREX Publication, pp: 23-35, 2022.

[4] Pankaj Agrawal, Bharat Mishra, Akhilesh Tiwari, "Effect of Parallel Capacitor in Matching Network of RF Energy Harvesting Circuit", International Journal of Electrical and Electronics Research (IJEER) , Volume 7, Issue 4, Pp:19-24, 2019.

[5] T. Starner, "Human-powered wearable computing," in IBM Systems Journal, vol. 35, no. 3.4, pp. 618-629, 1996.

[6] BapiDebnath and R. Kumar, "A Comparative Simulation Study of the Different Variations of PZT Piezoelectric Material by Using AMEMS Vibration Energy Harvester", IEEE Transactions on Industry Applications, VOL. 58, NO. 3, 2022.

[7] L. Xu, S. Zhou, Y. Xiang and Y. Yang, "Electromechanical finite element analysis for designed low-frequency MEMS piezoelectric vibration energy harvester," 2020 IEEE 70th Electronic Components and Technology Conference (ECTC), 2020, pp. 2112-2117, doi: 10.1109/ECTC32862.2020.00327.

[8] Geetha P, and H. D. Praveena, "Finite Element Method based Modelling and Study of the Electrical Characteristics of Nano MOSFET for Carbon Capture", Design Engineering, vol. 2021. No. 8, 2021.

[9] K. A. A. Wahib, Y. Wahab, A. Y. M. Shakaff, and S. Saadon, "Array design consideration of the MEMS vibration energy harvester cantilever-based structure: Top proof mass Vs back etch mass vs interdigitated electrode design," in Proc. IEEE Student Symp. Biomed. Eng. Science, pp. 64-69, 2015.

[10] B. H. J. Elyes, B. Marwa and D. Chérif, "Improvement of the UV light sensors modeling numerical platform performances," 2022 IEEE International Conference on Design & Test of Integrated Micro & Nano-Systems (DTS), pp. 01-06, 2022.

[11] Sil, I., B. Chakraborty, K. Dutta, H. Awasthi, S. Goel, and P. Bhattacharyya. "Capacitive Mode Vapor Sensing Phenomenon in ZnO Homojunction: An Insight Through Space Charge Model and Electrical Equivalent Circuit." IEEE Sensors Journal 22, no. 10 (2022): 9483-9490.

[12] T. T. Daniel, V. K. S. Yadav, E. E. Abraham and R. P. Paily, "Carbon Monoxide Sensor Based on Printed ZnO," in IEEE Sensors Journal, vol. 22, no. 11, pp. 10910-10917, 1 June 1, 2022.

[13] Khan Azam Hussain, Mushtaque Nur, and Omer Willander, Magnus, "Mechanical and piezoelectric properties of zinc oxide nanorods grown on conductive textile fabric as an alternative substrate", Journal of Physics D: Applied Physics. Vol.47. pp.345102, 2014.

[14] P. Geetha and R. S. D. Wahida Banu, "A compact modelling of double-walled gate wrap around carbon nanotube array field effect transistor", Journal of Computational Electronics, vol.13, No.4, pp. 900-916, 2014.

[15] Javid Basha Shaik and P. Venkatramana, "Investigation of Crosstalk Issues for MWCNT Bundled TSVs in Ternary Logic", ECS Journal of Solid State Science and Technology, Volume 11, Number 3, Electrochemical Society ("ECS"), 2022.

[16] S. Rani and J. Kumar, "Effect of Mg-doped zinc oxide nanoparticles as inorganic electron transport layer in quantum dot light-emitting diodes," 2022 Workshop on Recent Advances in Photonics (WRAP), pp. 1-2, 2022.



© 2022 by the Geeta P. Submitted for possible open access publication under the terms and conditions of the Creative Commons Attribution (CC BY) license <http://creativecommons.org/licenses/by/4.0/>.